

Defect-Induced Photoluminescence from Dark Excitonic States in Individual Single-Walled Carbon Nanotubes

Hayk Harutyunyan,^{*,†} Tobias Gokus,[‡] Alexander A. Green,[§] Mark C. Hersam,[§] Maria Allegrini,[†] and Achim Hartschuh[‡]

Dipartimento di Fisica "E. Fermi", Università di Pisa and CNISM, Largo Pontecorvo 3, 56127 Pisa, Italy, Department Chemie and Biochemie and CeNS, Ludwig-Maximilians-Universität München, 81377 München, Germany, and Department of Materials Science and Engineering, Department of Chemistry, Northwestern University, Evanston, Illinois 60208-3108

Received January 27, 2009; Revised Manuscript Received March 13, 2009

ABSTRACT

We show that new low-energy photoluminescence (PL) bands can be created in the spectra of semiconducting single-walled carbon nanotubes by intense pulsed excitation. The new bands are attributed to PL from different nominally dark excitons that are "brightened" because of a defect-induced mixing of states with different parity and/or spin. Time-resolved PL studies on single nanotubes reveal a significant reduction of the bright exciton lifetime upon brightening of the dark excitons. The lowest-energy dark state has longer lifetimes and is not in thermal equilibrium with the bright state.

Because of their exceptional electronic properties, single-walled carbon nanotubes (SWNTs) are promising candidates for future nanoelectronic and biosensing applications, as well as narrow-band nanoscale emitting and detecting devices.¹⁻⁴ Excitons are identified to dominate the absorption and PL emission properties of these one-dimensional systems.^{5,6} Enhanced electron-electron interactions due to the reduced dimensionality lead to exceptionally large binding energies of the excitons that are shown to exist even in metallic SWNTs.⁷ Theory predicts a manifold of excitonic bands below the free electron-hole continuum of semiconducting SWNTs.⁸⁻¹¹ Besides the optically active odd-parity singlet excitons, additional even-parity dipole-forbidden singlet excitons as well as triplet excitons are expected to occur. Most importantly, some of these bands form nonemissive states that are lower in energy than the lowest bright state. This complex sequence of excitonic states, and the nonradiative relaxation channels associated with them, presumably have an important impact on the low PL quantum yield of SWNTs and fast exciton decay rates.¹²⁻¹⁴ Therefore, detailed studies of the properties of dark excitonic states are essential

both for full understanding of the excited-state dynamics and for engineering of the optical properties of the SWNTs.

The direct experimental proof for the existence of dark excitonic states in SWNTs was presented, applying two-photon photoluminescence excitation spectroscopy^{5,6} and measurements of magnetic brightening of the SWNT PL.¹⁵ Low-energy forbidden states were also used to explain the dynamics observed in pump-probe experiments^{16,17} and the temperature dependence of PL intensities.¹⁸ In addition, recent results on ensemble¹⁹ and individual nanotube samples²⁰ have shown low-energy satellite peaks in the PL spectra. These peaks were attributed to emission from low-lying dark excitonic states, while the mechanisms that enable optically forbidden transitions and the interplay between bright and dark excited states remain to be clarified.

In this Letter, we report on the creation of low-energy emission bands in the PL spectra of individual (5,4) and (6,4) SWNTs upon high-power pulsed-laser irradiation at room temperature. The persistence of these bands in subsequent low-power measurements indicates that irreversible distortions of the nanotube structure efficiently "brighten" forbidden states via disorder-induced mixing of excitonic states, in agreement with theoretical predictions.^{9,21} The clear distinction between additional emissive features belonging to a certain nanotube and PL bands from other nanotubes is made possible by observing single nanotube spectra before and after high-power irradiation and by recording the

* Authors to whom correspondence should be addressed. E-mail: Hayk@df.unipi.it, achim.hartschuh@cup.uni-muenchen.de.

[†] Dipartimento di Fisica "E. Fermi", Università di Pisa and CNISM.

[‡] Department Chemie and Biochemie and CeNS, Ludwig-Maximilians-Universität München.

[§] Department of Materials Science and Engineering, Department of Chemistry, Northwestern University.

polarization dependence of bright and dark emission bands. While the decay times of the allowed transition are in the range of 1–40 ps,²² much-longer dark-state lifetimes of up to 177 ps have been observed. Based on the spectroscopic properties of the lowest dark-state emission and its observation upon nanotube exposure to gold that is predicted to create high local spin densities,^{23,24} we suggest that low-energy emission results from triplet exciton recombination facilitated by magnetic defects and impurities.

Time-correlated single-photon counting (TCSPC) is used, in combination with confocal microscopy, to perform single SWNT spectroscopy and time-resolved PL measurements.²² Spatially isolated individual SWNTs were obtained by spin-coating a small volume of micelle-encapsulated CoMoCat material onto a glass coverslip.²⁵ The typical nanotube length determined by AFM measurements was $\sim 550 \pm 150$ nm. Laser excitation was provided by a Ti:sapphire oscillator operated at a photon energy of 1.63 eV, a repetition rate of 76 MHz, and a pulse duration of ~ 150 fs. The inverted confocal microscope, combined with a high numerical aperture objective (NA = 1.3), provided a diffraction-limited excitation spot of ~ 400 nm and a maximum collection efficiency required for single nanotube detection. The PL spectra were recorded with a CCD camera, and a fast avalanche photodiode was used to acquire PL transients. The instrument response function (IRF) of the system was independently measured by detecting the scattered pump laser light from the sample and had a full width at half-maximum (fwhm) of 27 ps. Because of the high signal-to-noise ratio achieved in our experiments and the reproducibility of the IRF, the time resolution of the setup is ~ 3 ps, which is close to 10% of the fwhm of the IRF.¹³

Figure 1 shows the generation of low-energy satellite PL bands for two individual nanotubes. Initial spectra (black lines) acquired at low excitation intensity ($I_0 = 3 \times 10^{13}$ photons pulse⁻¹ cm⁻²) show a single emission peak centered at 1.41 eV (Figure 1a) and 1.46 eV (Figure 1b) assigned to the allowed bright exciton (BE) in (6,4) and (5,4) nanotubes, respectively.²⁶ Irradiation of the nanotubes for 10–100 s with an order-of-magnitude-higher pulse intensity of $\sim 17 \times I_0$ results, in some cases, in significantly modified spectra (denoted by the red lines in Figure 1) with additional red-shifted shoulders and new spectral features transferring substantial spectral weight to these satellite peaks. Importantly, no such spectral changes were induced at the corresponding averaged power levels using continuous-wave (cw) excitation, suggesting that high pulse intensities that initiate multiphoton processes are crucial to induce these modifications. High-power cw excitation, on the other hand, mainly leads to the photobleaching and blinking of nanotube PL.²⁷ Satellite peaks for different (6,4) and (5,4) nanotubes consistently appear at similar energies and can be roughly divided into two groups, with red shifts of ~ 110 –190 meV (DE₁) and ~ 30 –60 meV (DE₂), in good agreement with ref 20. The same energy splittings (130 and 40 meV) were predicted for the (6, 4) nanotube and attributed to triplet and even-parity singlet excitons, respectively.¹¹

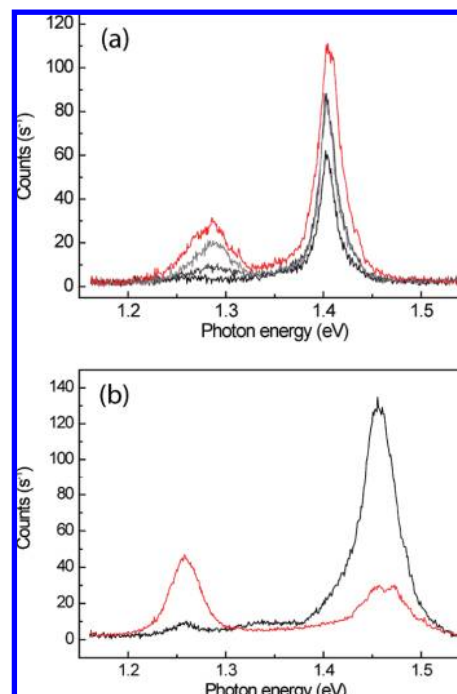


Figure 1. Creation of low-energy satellite peaks in the PL spectrum of (a) a (6,4) SWNT and (b) a (5,4) SWNT. Initial spectra (black lines) acquired at low excitation intensity ($I_0 = 3 \times 10^{13}$ photons pulse⁻¹ cm⁻²) and considerably modified spectra (red lines) of the same nanotubes acquired at $\sim 17 \times I_0$ for (a) and I_0 for (b) after exposure to high excitation intensity ($\sim 17 \times I_0$). Low-energy satellite contributions shifted by ~ 30 –60 meV (DE₂) and ~ 110 –190 meV (DE₁), with respect to the bright exciton emission, are assigned to emission from optically dark states. Gray lines in panel (a) were acquired sequentially between initial and final spectrum at intermediate intensity ($\sim 7 \times I_0$), illustrating the steplike creation of the additional bands.

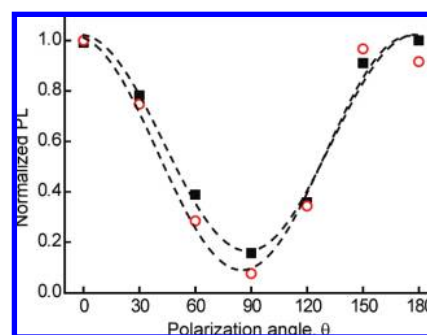


Figure 2. Polarization dependence of the PL emission for (○) the bright exciton (BE) and (■) the dark exciton DE₁, determined from a series of spectra recorded for the same (6,4) nanotube. The dashed lines are $\cos^2 \theta$ fits.

The polarization analysis of PL emission of the original bright exciton peak and the newly created satellite DE₁ (Figure 2) exhibit the same $\cos^2 \theta$ behavior, proving that the emission bands belong to the same nanotube and indicating that the red-shifted emission originates from an intrinsic state of the SWNT. Furthermore, the consistent appearance of the new bands in DNA-wrapped SWNTs and nanotubes embedded in a poly(methyl methacrylate) (PMMA) matrix (see Figure S1 in the Supporting Information) shows that the effect is not due to a chemical reaction that is specific to the

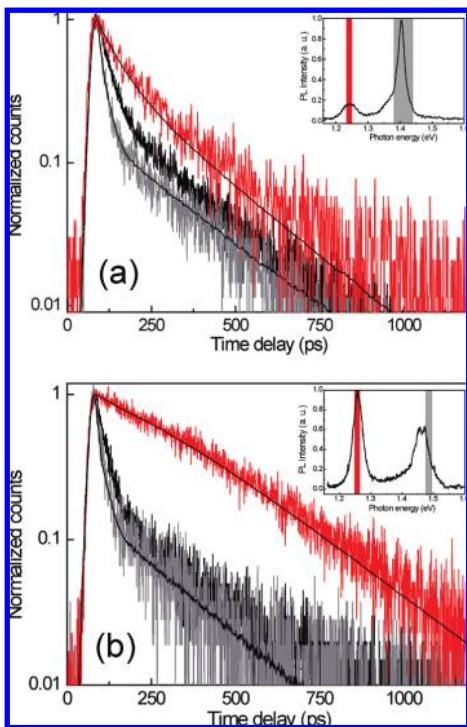


Figure 3. Semilogarithmic plot of the PL transients visualizing the decay dynamics of different emission peaks in the spectra of individual SWNT (insets) for two different chirality nanotubes: (a) (6,4) and (b) (5,4). Black curves show the decay of the BE state detected in the gray-shaded spectral range in the insets before the creation of the low-energy satellites. After creation of the dark-state emission the decay rate of the bright exciton is increased significantly (gray lines). The decay of the dark excitonic state DE_1 , shifted by 110–190 meV, with respect to the BE, is substantially slower (red curves). PL decay traces detected for smaller shifts of 30–60 meV resulting from DE_2 are identical to those of the bright exciton (data not shown). Dashed lines are exponential fits to the data (see text).

sodium cholate surfactant. Furthermore, the different population dynamics of BE and DE_1 states (vide infra) excludes the possibility of shifted singlet emission that is due to, for example, a sudden change in the dielectric constant of the environment.

Based on these experimental observations, we conclude that, during the intense irradiation, the structure of the nanotube is modified by the creation of local defect sites. These defects alter the local symmetry of the nanotube partially removing restrictions for the population and subsequent emission from intrinsic dark states.⁹

To determine the population dynamics of both dark and bright excitonic states, and to study the effect of the created disorder, we have performed time-resolved PL measurements of the different emission bands before and after the creation of emission satellites. Figure 3 depicts representative PL transients detected from the shaded spectral areas (shown in the insets) for two individual nanotubes of two different chiralities: (6,4) (Figure 3a) and (5,4) (Figure 3b). Two important conclusions can be drawn from these data. First, upon creation of the satellite peaks, the bright exciton lifetime is decreased (gray curve), compared to the initial decay (black curve); second, the DE_1 emission has a much longer decay

time. Monoexponential fits (represented by dashed lines in the figure) to these transients give the lifetimes of the main emission peaks before and after creation of the red-shifted band of 20 and 6 ps for the (6,4) nanotube (Figure 3a) and 13 and 2 ps for the (5,4) tube (Figure 3b), respectively. The emission bands with smaller energy shifts in the range of several tens of meV (DE_2) exhibit exactly the same decay behavior as the main peak (data not shown). Dark states a few meV below the bright exciton were shown to affect the dynamics of BE PL.¹⁴ The observed slow decay component was attributed to weak coupling of the two states. This study, focusing on highly luminescent and presumably defect-free individual nanotubes, explained the inefficient coupling to be mediated by phonon modes. Assuming that the DE_2 observed here is identical to that of ref 14, its similar dynamics with the BE indicates that, because of the defect-induced mixing of the excitonic states, the efficiency of the coupling is significantly increased, leading to faster transition rates and thermal equilibration between the two states. The decay of dark exciton DE_1 is dominated by much longer time constants: 65 and 177 ps for the (6,4) and (5,4) nanotubes, respectively, in the present example. Thus, other origins of the low-energy bands, such as biexcitons and phonon replica of the bright exciton, can be ruled out, based on this slow decay dynamics. In addition, we observed a fast decay component (8 and 2 ps) with a much-smaller photon flux (by a factor of $\sim 1/20$). This component is either due to transitions from DE_1 to BE or to other dark excitonic states within the DE_1 manifold. Generally, the decay dynamics of DE_1 is expected to be complex and difficult to assess, because the defects responsible for the brightening will be localized, presumably affecting only finite-length nanotube sections on the order of the exciton's diffusional range (~ 110 nm).^{27,32} Because of the large separation of the emission peaks and the detected spectral windows (shaded areas in insets in Figure 3), overlapping emission contributions from the BE state are not sufficient to explain this decay component. Measurements on several other (6,4) and (5,4) SWNTs consistently show the same effects with DE_1 lifetimes ranging up to 177 ps. Decay times derived from time-resolved PL and pump-probe data in the range of 50–300 ps with small relative amplitudes have been reported previously^{28,29} from ensemble samples as part of multiexponential decay. We speculate that these decay times could originate from the newly created states observed here.

Now we discuss the more rapid decay of the bright exciton in the presence of the red-shifted peaks (Figure 3). Because the amplitude of the BE peak is decreased, we conclude that disorder-inducing defects are responsible for additional radiationless relaxation channels depopulating the bright excitonic state. Two possible competing channels can be distinguished. First, population transfer to the dark state DE_1 , mediated by the introduced defects and second, decays to the ground state, facilitated by enhanced exciton-phonon coupling, because of defect-associated local phonon modes.^{30,31} Both relaxation channels require propagation of the bright exciton along the nanotube to enable interaction with localized defects; therefore, faster decay also serves as

an evidence for the mobility of excitons in nanotubes.^{13,27,32} Population transfer from bright states to dark states, on the other hand, would result in a delayed rise of the DE₁ emission with a rise time that is equal to the decay time of the bright state. Such a delayed rise, which would be detectable in our measurements, especially for nanotubes with longer decay times of the BE state of up to 25 ps, was not observed, suggesting that a substantial fraction of the dark state population is built up directly upon photoexcitation. Importantly, the fact that the bright exciton maintains a different and finite lifetime in the presence of the dark state DE₁ clearly shows that these two states are not in thermal equilibrium.

Finally, the most intriguing issue of the novel emission is the nature of the excitonic state that is responsible for it. The strongly polarized emission of the DE₁ state depicted in Figure 2 and its regular appearance at similar emission energies for different nanotubes makes the possibility of simply having luminescent defects unlikely. Recent experimental studies on ensemble samples enriched with (6,5) chirality nanotubes have attributed low-energy emission bands to 160 meV phonon sidebands of K momentum excitons that are higher in energy than the BE.³³ However, the large energy separation of the DE₁ state of ~190 meV observed in the present work (Figure 1b) also excludes this scenario. On the other hand, the energy separation for the triplet state calculated for the (6,4) chirality in ref 11 is in good agreement with our experimental data. The intersystem crossing leading to triplet emission can be assisted by coupling to high spin density states created by sidewall modification of the nanotube, such as vacancy creation.^{34,35} The energy of ~5 eV needed to create a vacancy³⁴ can be provided through multiphoton excitation processes, which explains the high pulse energies required for the creation of DE₁. Generally, magnetic impurities that increase spin–orbit coupling could also be formed by trace amounts of residual catalyst materials, which explains the observation of dark state emission in other nanotube materials reported in the literature.^{19,20,36} The slow PL decay times for the triplet exciton can be explained by the spin-dependent nature of the nonradiative relaxation mechanism.

To test this possibility, we treated the SWNTs with a pH-neutralized aqueous solution of gold that induces spin-polarized states with significant magnetic moments when adsorbed on SWNTs²³ or graphene surfaces.²⁴ Strikingly, covering the sample with a gold solution results in similar changes in the single nanotube PL spectrum without requiring high-power pulsed excitation (see Figure S2 in the Supporting Information), thus supporting the hypothesis of the triplet state emission. The efficiency of brightening of the dark states is especially high when the aqueous SWNTs solution is premixed with the gold solution before deposition, thus facilitating the surface adsorption of the metal. In these samples, the majority of the (6, 4) nanotubes exhibited red-shifted emission satellites at similar energies, indicating that the same emissive DE₁ state is brightened. This has been further confirmed by time-resolved measurements showing a broad distribution of lifetimes in the range of 7–150 ps,

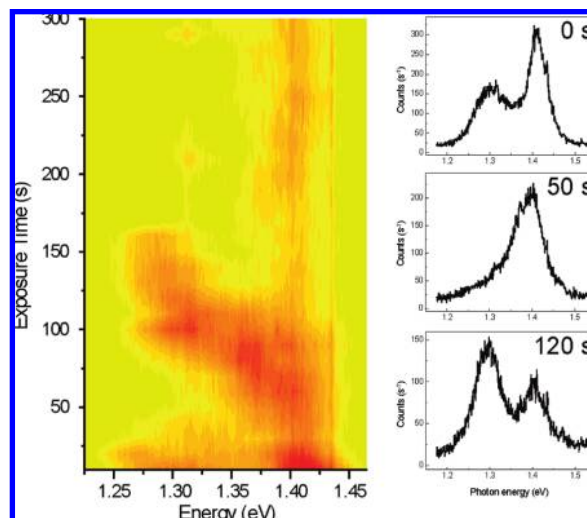


Figure 4. Series of PL spectra from a (6,4) SWNT after treatment with the gold solution. The series show the temporal evolution of the emission with blinking and spectral shifts under low-power cw excitation. The characteristic emission of DE₁ at ~1.28 eV varies with time and can be observed here in the time intervals of 0–40 s and 100–160 s. This type of behavior was determined to be characteristic for nanotubes treated with gold solution and is possibly due to the mobility of the adsorbed Au atoms on the nanotube surface.

which is considerably longer than that for the BE emission. However, there is a noteworthy difference between the two methods of “brightening” of the dark states. As shown in Figure 4, after the gold treatment, the DE₁ emission is far less stable, even under low-power cw excitation, showing pronounced spectral shifting and blinking. Possibly, the mobility of the adsorbed Au atoms on the nanotube surface is causing the unstable interaction with the nanotube and the varying spectral characteristics.³⁷ Importantly, no additional PL bands have been observed in control experiments on single nanotubes that have been deposited on gold films (not shown) as well as near-field optical experiments using sharp gold tips,³⁸ indicating that the new PL bands are not created by metal-surface-induced electromagnetic field enhancement.

In conclusion, we demonstrated that nominally dark excitonic states in carbon nanotubes can become emissive after exposure to high excitation intensities and by adsorption of gold. We suggest that local defects induce the mixing of different excitonic states and the relaxation of selection rules via perturbation of the electronic structure. Our single nanotube measurements show that the recombination time of the excitons can be modified by the presence of disorder and that PL from the same nanotube can have decay rates varying by 2 orders of magnitude, depending on the detected spectral range. Although these findings are relevant for nanotube photophysics, they also indicate possible novel routes for the engineering of SWNT optical properties.

Acknowledgment. We thank Nicolai Hartmann for valuable experimental help. Financial support by the DFG (through Grant No. HA4405/4-1 and Nanosystem Initiative München (NIM)) is gratefully acknowledged. This work was also funded by the U.S. National Science Foundation

(under Award Nos. DMR-0520513, EEC-0647560, and DMR-0706067). H.H. acknowledges the financial support from the School of Graduate Studies G. Galilei (University of Pisa).

Supporting Information Available: PL spectra of a DNA-wrapped (6,4) SWNT covered by PMMA showing the creation of low-energy-emission satellites upon high power irradiation (Figure S1), and PL spectra of an individual (6,4) SWNT before and after exposure to gold solution (Figure S2). This material is available free of charge via the Internet at <http://pubs.acs.org>.

References

- (1) Jorio, A.; Dresselhaus, M. S.; Dresselhaus, G., Eds. *Carbon Nanotubes; Topics in Applied Physics*, Vol. 111; Springer: Berlin/Heidelberg, 2008.
- (2) Lu, W.; Lieber, C. M. *Nat. Mater.* **2007**, *6*, 841.
- (3) Barone, P. W.; Seunghyun, B.; Heller, D. A.; Strano, M. S. *Nat. Mater.* **2004**, *4*, 86.
- (4) Leeuw, T. K.; Reith, R. M.; Simonette, R. A.; Harden, M. E.; Cherukuri, P.; Tsybolski, D. A.; Beckingham, K. M.; Weisman, R. B. *Nano Lett.* **2007**, *7*, 2650.
- (5) Wang, F.; Dukovic, G.; Brus, L. E.; Heinz, T. F. *Science* **2005**, *308*, 838.
- (6) Maultzsch, J.; Pomraenke, R.; Reich, S.; Chang, E.; Prezzi, D.; Ruini, A.; Molinari, E.; Strano, M. S.; Thomsen, C.; Lienau, C. *Phys. Rev. B* **2005**, *72*, 241402(R).
- (7) Wang, F.; Cho, D. J.; Kessler, B.; Deslippe, J.; Schuck, P. J.; Louie, S. G.; Zettl, A.; Heinz, T. F.; Shen, Y. R. *Phys. Rev. Lett.* **2007**, *99*, 227401.
- (8) Zhao, H.; Mazumdar, S. *Phys. Rev. Lett.* **2004**, *93*, 157402.
- (9) Perebeinos, V.; Tersoff, J.; Avouris, P. *Nano Lett.* **2005**, *5*, 2495.
- (10) Tretiak, S. *Nano Lett.* **2007**, *7*, 2007.
- (11) Chang, E.; Prezzi, D.; Ruini, A.; Molinari, E. arXiv:cond-mat/0603085v1.
- (12) Wang, F.; Dukovic, G.; Brus, L. E.; Heinz, T. F. *Phys. Rev. Lett.* **2004**, *92*, 177401.
- (13) Hagen, A.; Steiner, M.; Raschke, M. B.; Lienau, C.; Hertel, T.; Qian, H.; Meixner, A. J.; Hartschuh, A. *Phys. Rev. Lett.* **2005**, *95*, 197401.
- (14) Berciaud, S.; Cognet, L.; Lounis, B. *Phys. Rev. Lett.* **2008**, *101*, 077402.
- (15) Srivastava, A.; Htoon, H.; Klimov, V. I.; Kono, J. *Phys. Rev. Lett.* **2008**, *101*, 087402.
- (16) Zhu, Z.; Crochet, J.; Arnold, M. S.; Hersam, M. C.; Ulbricht, H.; Resasco, D.; Hertel, T. *J. Phys. Chem. C* **2007**, *111*, 3831.
- (17) Seferyan, H. Y.; Nasr, M. B.; Senekerimyan, V.; Zadoyan, R.; Collins, P.; Apkarian, V. A. *Nano Lett.* **2006**, *6*, 1757.
- (18) Mortimer, I. B.; Nicholas, R. J. *Phys. Rev. Lett.* **2007**, *98*, 027404.
- (19) Metzger, W. K.; McDonald, T. J.; Engrakul, C.; Blackburn, J. L.; Scholes, G. D.; Rumbles, G.; Heben, M. J. *J. Phys. Chem. C* **2007**, *111*, 3601.
- (20) Kiowski, O.; Arnold, K.; Lebedkin, S.; Hennrich, F.; Kappes, M. M. *Phys. Rev. Lett.* **2007**, *99*, 237402.
- (21) Spataru, C. D.; Ismail-Beigi, S.; Capaz, R. B.; Louie, S. G. *Phys. Rev. Lett.* **2005**, *95*, 247402.
- (22) Gokus, T.; Hartschuh, A.; Harutyunyan, H.; Allegrini, M.; Hennrich, F.; Kappes, M.; Green, A. A.; Hersam, M. C.; Araújo, P. T.; Jorio, A. *Appl. Phys. Lett.* **2008**, *92*, 153116.
- (23) Durgun, E.; Dag, S.; Ciraci, S.; Gulseren, O. *J. Phys. Chem. B* **2004**, *108*, 575.
- (24) Krashenninnikov, A. V.; Foster, A. S.; Nieminen, R. M. *NT08 Conference, Book of Abstracts*, 2008; p 52.
- (25) Green, A. A.; Hersam, M. C. *Mater. Today* **2007**, *10*, 59.
- (26) Bachilo, S. M.; Strano, M. S.; Kittrell, C.; Hauge, R. H.; Smalley, R. E.; Weisman, R. B. *Science* **2002**, *298*, 2361.
- (27) Georgi, C.; Hartmann, N.; Gokus, T.; Green, A. A.; Hersam, M. C.; Hartschuh, A. *ChemPhysChem* **2008**, *9*, 1460.
- (28) Berger, S.; Voisin, C.; Cassabois, G.; Delalande, C.; Roussignol, P. *Nano Lett.* **2007**, *7*, 398.
- (29) Huang, L.; Pedrosa, H. N.; Krauss, T. D. *Phys. Rev. Lett.* **2004**, *93*, 017403.
- (30) Habenicht, B. F.; Kamisaka, H.; Yamashita, K.; Prezhdo, O. V. *Nano Lett.* **2007**, *7*, 3260.
- (31) Perebeinos, V.; Avouris, P. *Phys. Rev. Lett.* **2008**, *101*, 057401.
- (32) Cognet, L.; Tsybolski, D. A.; Rocha, J. D. R.; Doyle, C. D.; Tour, J. M.; Weisman, R. B. *Science* **2007**, *316*, 1465.
- (33) Torrens, O. N.; Zheng, M.; Kikkawa, J. M. *Phys. Rev. Lett.* **2008**, *101*, 157401.
- (34) Lehtinen, P. O.; Krashenninnikov, A. V.; Foster, A. S.; Nieminen, R. M. *Carbon Based Magnetism*; Elsevier: Amsterdam, 2006.
- (35) Lehtinen, P. O.; Foster, A. S.; Ayuela, A.; Krashenninnikov, A.; Nordlund, K.; Nieminen, R. M. *Phys. Rev. Lett.* **2003**, *91*, 017202.
- (36) Lefebvre, J.; Finnie, P.; Homma, Y. *Phys. Rev. B* **2004**, *70*, 045419.
- (37) Gan, Y.; Sun, L.; Banhart, F. *Small* **2008**, *4*, 587.
- (38) Qian, H.; Araújo, P. T.; Georgi, C.; Gokus, T.; Hartmann, N.; Green, A. A.; Jorio, A.; Hersam, M. C.; Novotny, L.; Hartschuh, A. *Nano Lett.* **2008**, *8*, 2706.

NL9002798